RESEARCH ARTICLE SUMMARY

BIOMECHANICS

The principles of cascading power limits in small, fast biological and engineered systems

Mark Ilton, M. Saad Bhamla,* Xiaotian Ma,* Suzanne M. Cox,* Leah L. Fitchett, Yongjin Kim, Je-sung Koh, Deepak Krishnamurthy, Chi-Yun Kuo, Fatma Zeynep Temel, Alfred J. Crosby, Manu Prakash, Gregory P. Sutton, Robert J. Wood, Emanuel Azizi,† Sarah Bergbreiter,† S. N. Patek†‡

INTRODUCTION: Mechanical power, whether for launched missiles or running humans, is limited by the universal, physical trade-off between force and velocity. However, many biological systems use power-amplifying mechanisms that enable unmatched accelerations in challenging environments and across a wide range of size scales. How these mechanisms actually enhance power output remains unclear. Power-amplified biological systems are of particular interest because they achieve a trio of combined capabilities that exceed current engineering performance: (i) high accelerations that (ii) can be continuously fueled through metabolic processes and (iii) are used repeatedly with minimal performance degradation throughout the life of the organism. Although engineers have struggled to design lightweight and long-lasting devices that can deliver high power output, biological systems have been performing such feats for millions of years and using these systems for a myriad of functions.

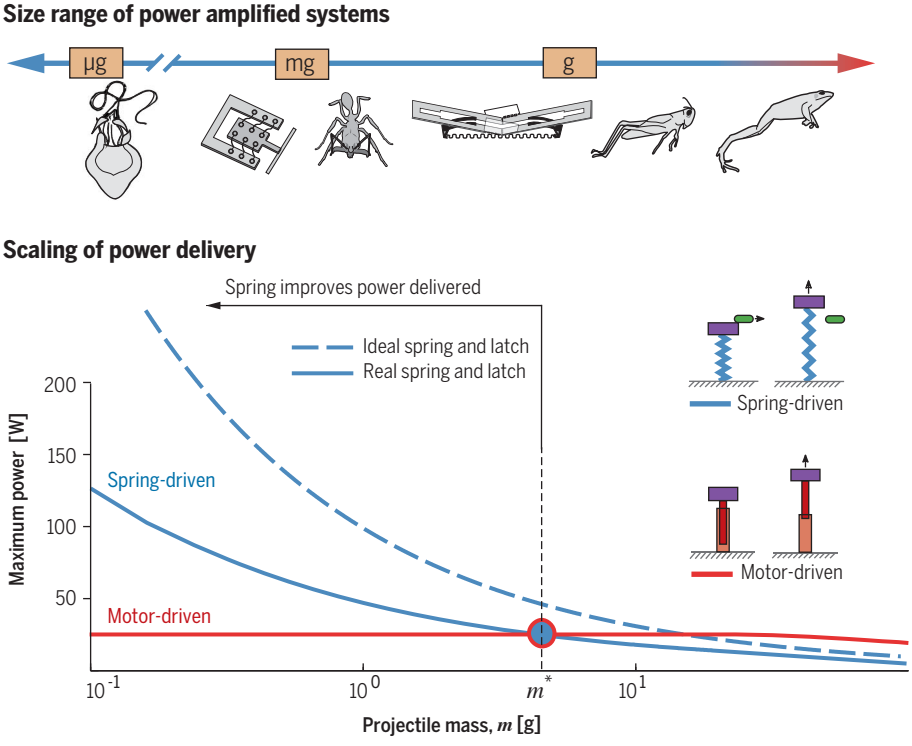

Power-amplified biological and synthetic systems use spring elements to drive motion over a range of size scales. Mathematical modeling reveals a cascade of power limits and mass-dependent transitions in power delivery that arise from the integration of motors, springs, and latches to actuate movement. Variation of these components creates synergistic effects relevant to the analysis and synthesis of diverse power-amplified systems.

RATIONALE: Through a mathematical analysis that is equally applicable to biological and synthetic systems, we investigate how power enhancement emerges through the dynamic coupling of motors, springs, latches, and projectiles and relate the findings to data on existing biological and engineered systems. The model incorporates nonideal behavior of spring and latch systems in a scalable framework using both dimensional and dimensionless approaches.

RESULTS: Motors, springs, and latches all experience force-velocity trade-offs, and their integration exemplifies the cascading effects of power limits. Springs circumvent motor power limits when projectile mass is small and the motor's force-velocity dynamics limit performance. However, springs also exhibit force-velocity trade-offs when their mass, mechanical properties, and time dependence are incorporated. Latches dynamically modulate spring power through variation in latch shape and velocity. Motor-driven and spring-driven movements are distinct in their transitions across performance (power, maximum velocity, and duration), which are largely dictated by projectile mass. When analyzed as a single, integrated system, the necessity for tuning and inherent tunability are evident. Simply increasing the force output of a motor does not enhance performance; the spring and latch capacities must also shift. Simply decreasing the size of the system also does not enhance performance; spring energy storage falls off at smaller scales due to the effects of materials, stiffness, and geometry. With this mathematical foundation of scaling and integration, we apply a new lens to patterns of biological scaling limits and propose new design principles for integrated and tuned systems.

ON OUR WEBSITE

Read the full article at http://dx.doi.org/10.1126/science.aao1082

CONCLUSION: Our model reveals a foundational framework for the scaling, synthetic design, and evolutionary diversification of power-amplified systems. The model enables a straightforward approach to analyzing biological systems, encourages a rich design space and functionality for synthetic systems, and highlights a compelling need for the integrative analysis of spring and latch dynamics in both synthetic and biological systems. ■

The list of author affiliations is available in the full article online.
*These authors contributed equally to this work.
†These authors contributed equally to this work.
‡Corresponding author. Email: snp2@duke.edu (S.N.P.)
Cite this article as M. Ilton *et al.*, *Science* **360**, eaao1082 (2018). DOI: 10.1126/science.aao1082

RESEARCH ARTICLE

BIOMECHANICS

The principles of cascading power limits in small, fast biological and engineered systems

Mark Ilton,[1] M. Saad Bhamla,[2]*† Xiaotian Ma,[3]* Suzanne M. Cox,[4]* Leah L. Fitchett,[4] Yongjin Kim,[1] Je-sung Koh,[5]‡ Deepak Krishnamurthy,[2] Chi-Yun Kuo,[4]§ Fatma Zeynep Temel,[5] Alfred J. Crosby,[1] Manu Prakash,[2] Gregory P. Sutton,[6] Robert J. Wood,[5] Emanuel Azizi,[7]|| Sarah Bergbreiter,[3]|| S. N. Patek[4]||¶

Mechanical power limitations emerge from the physical trade-off between force and velocity. Many biological systems incorporate power-enhancing mechanisms enabling extraordinary accelerations at small sizes. We establish how power enhancement emerges through the dynamic coupling of motors, springs, and latches and reveal how each displays its own force-velocity behavior. We mathematically demonstrate a tunable performance space for spring-actuated movement that is applicable to biological and synthetic systems. Incorporating nonideal spring behavior and parameterizing latch dynamics allows the identification of critical transitions in mass and trade-offs in spring scaling, both of which offer explanations for long-observed scaling patterns in biological systems. This analysis defines the cascading challenges of power enhancement, explores their emergent effects in biological and engineered systems, and charts a pathway for higher-level analysis and synthesis of power-amplified systems.

Certain organisms are renowned for their ability to circumvent the force-velocity trade-off of muscle motors through mechanisms of power amplification that greatly reduce the amount of time required to perform a given amount of work (force × velocity = work/time = power) (*1*–*3*). Numerous studies have explored muscular power output and the underlying force-velocity trade-offs (*4*, *5*), as well as the enhanced power output achieved using springs and latches (*6*–*11*); however, these studies have yet to fully explain the limits of mass-specific power output [power density (W/kg)] in these organisms. For example, in many of these systems, the motor does work to store energy in a spring, and then the spring solely actuates the motion. The spring serves as the actuator for the system and, therefore, must operate under its own mass-specific power limits analogous to the motor; however, the power densities of elastic materials are largely unknown for biological and synthetic systems.

We investigate how nonidealized components of power-amplified systems, such as springs and latches, enhance and mediate power output. We apply a modeling approach that is grounded in a simplified power amplification system (Fig. 1), which delineates the limits, integration, and scaling of these systems. Our goal is to formulate the fundamental interactions of mechanical power amplification that apply to both engineered and biological systems. The model is used to successively investigate the role of motors, springs, and latches in mechanical power amplification by addressing four central questions: (i) Under which inertial-loading conditions is a projectile best launched by a motor versus a spring? (ii) What are the implications of spring force-velocity behavior for the generation of power amplification? (iii) How do latches mediate the dynamics of energy release? and (iv) What are the general principles of integrated tuning for power-amplified systems? As we answer each guiding question, we place the findings into an interdisciplinary context and explain trends and limits in existing systems.

A foundational lesson from archery

Archery illustrates the benefits and limits of power amplification that emerge from the integration of a motor, spring, and latch. Arm muscles serve as motors that put energy into the bow (the spring). Fingers act as latches that resist the release of the elastic energy stored in the bow and determine the timing of energy delivery from the bow to the arrow. The arrow is launched solely by the bow's stored elastic energy. The addition of a bow has two distinct benefits. First, the bow decouples the arm muscles from the arrow's launch, such that the muscles need not contract quickly. Instead, the muscles contract slowly and forcefully to load the stiff spring. Second, the bow can launch the lightweight arrow without the inertial load of the arm, resulting in higher velocity, kinetic energy, and acceleration than if the arrow had been thrown. Even so, although it is sensible to launch a lightweight arrow with a bow, we would not reach for the same bow to launch a heavy stone. The projectile's size should determine whether the bow yields higher launching kinetic energy than possible from the arm alone (*12*). To optimize the system, the properties of the elastic bow should be tuned to the force capacity of the arm muscles and the fingers' ability to restrain the bow's release. Just as in archery, the hallmarks of biological power amplification are the spatial and temporal decoupling of motor and spring; the use of slow and forceful muscle contractions; the tuning of muscle, spring, and latch for maximum work capacity; and the reduction of inertial load (*6*, *7*, *13*).

The lessons from archery and their manifestation in biology set up a series of questions that we address sequentially, beginning with the major components of power amplification—motor, spring, and latch—and concluding with an analysis of their integration. We formulate a mathematical approach that is equally applicable to biological and synthetic systems. To achieve a general framework, we model the system in the simplest possible terms that enable dimensional (presented here) and dimensionless (see supplementary materials) analyses that define a parameter space for investigation and synthesis across systems and scales.

Launching with a motor versus a spring

Our mathematical model—consisting of a motor, spring, and latch—simulates the launch of projectiles of varying mass, m (see supplementary materials for details). A linear force-velocity relation for the motor is held constant during the simulation (Fig. 1A). We solve the dynamical equations of motion for a projectile launched either by the motor alone (Fig. 1B) or by a spring that is preloaded by that same motor (Fig. 1C). In this section, we focus on the question, Under which inertial-loading conditions is a projectile best launched by a motor versus a spring?

The simulation highlights a key transition between small masses, which can achieve high velocities through the addition of elastic elements, and large masses, which are constrained by their inertial loads (Fig. 2). The addition of a spring is beneficial under two scenarios, when (i) takeoff velocity of the projectile is limited by motor velocity and (ii) projectile mass is small. For motor-only actuation, if projectile mass, m, is low, then

[1]Department of Polymer Science and Engineering, University of Massachusetts Amherst, Amherst, MA 01003, USA. [2]Department of Bioengineering, Stanford University, Stanford, CA 94305, USA. [3]Department of Mechanical Engineering and Institute for Systems Research, University of Maryland, College Park, College Park, MD 20742, USA. [4]Department of Biology, Duke University, Durham, NC 27708, USA. [5]School of Engineering and Applied Sciences and Wyss Institute for Biologically Inspired Engineering, Harvard University, Cambridge, MA 02138, USA. [6]School of Biological Sciences, University of Bristol, Bristol BS8 1TH, UK. [7]Ecology and Evolutionary Biology, University of California Irvine, Irvine, CA, USA.
*These authors contributed equally to this work. †Present address: School of Chemical and Biomolecular Engineering, Georgia Institute of Technology, Atlanta, GA 30332, USA. ‡Present address: Department of Mechanical Engineering, Ajou University, Suwon, 16499, South Korea. §Present address: Division of Evolutionary Biology, Ludwig Maximilian University of Munich, Grosshaderner Strasse 2, 82152 Planegg-Martinsried, Germany. ||These authors contributed equally to this work.
¶Corresponding author. Email: snp2@duke.edu (S.N.P.)

takeoff velocity, v_{to}, is limited by the speed of the motor, as seen in the asymptotic approach to v_{max} as m approaches zero. When projectile mass is high, takeoff velocity is limited by the inertia of the projectile. For spring-driven actuation, takeoff velocity is not limited by the motor when the projectile mass is low, and the resulting takeoff velocity is much larger than in the motor-driven case. These findings are consistent with previous analyses of motor-spring systems (*12*).

Building on these classic findings, we investigate the effects of varying mass on kinematic performance. We find that the transition to effective spring actuation depends on the focal performance metric. If the goal is to maximize takeoff velocity, the transition occurs at a smaller projectile mass than if the focal metric is takeoff duration or maximum power output (Fig. 2).

The relationship between force capacity of a motor and stiffness of a spring determines the amount of stored elastic energy (*12*, *14*). This is important for biological systems because motor force capacity varies as a function of length scale. Biological motors used for power amplification maximize force development at the cost of loading velocity and do so at exclusively small inertial loads (Tables 1 and 2). Invertebrates such as trap-jaw ants and mantis shrimp use long sarcomeres (the contractile units of muscle) to generate slow but forceful contractions to load the elastic elements that subsequently power their extremely rapid movement (*15*, *16*). Plants such as Venus flytraps, aquatic bladderworts, and fern sporangia use slow and forceful nonmuscular hydraulic movements (or nastic movements) coupled with elastic instabilities to achieve rapid motion (*17*–*20*). For many power-amplified systems, loading energy into the spring often takes orders of magnitude longer than releasing the energy (*13*), exemplifying the trade-off of generating work (force × distance) through large forces and small displacements at the cost of velocity.

Force-velocity trade-offs of spring-driven systems are ubiquitous in engineered systems. Most engineered systems use electromagnetic motors with transmissions that generate large torques that slowly load spring elements (*21*–*31*). For small systems, a shape memory alloy (SMA) is chosen for its high specific force and linear actuation (*32*–*34*). This high specific force comes with low velocity: Heating and cooling the material above and below its phase transition temperature is time-consuming. Engineered power-amplified systems often propel larger inertial loads than biological systems (Tables 1 and 2). Still, some engineered jumping systems (Table 2) effectively use combustion, powerful pneumatic actuators, or high-power electromagnetic actuators that actuate directly without the use of power amplification (*29*, *30*, *35*–*40*).

Power of springs

Although the focus on power amplification has historically revolved around the force-velocity trade-off of motors, the dynamic behavior of springs delivers this power to the payload in spring-mass systems (*12*). Springs have typically been characterized in terms of force-displacement curves and defined by geometrical and material properties, while still leaving their potential for power enhancement unresolved (*41*, *42*). Furthermore, springs are typically assumed to operate as ideal structures without internal mass or dissipation, such that the energy put into a spring is equal to the energy leaving the spring. By this logic, a spring driving no load mass would accelerate infinitely quickly. Here, we examine how realistic spring actuators limit or enable power amplification. Building on the mathematical model of the previous section, in this section we ask, What are the implications of spring force-velocity behavior for the generation of power amplification? Given that springs have traditionally been assumed to be ideal, the force-velocity behavior and influence of the material and geometric properties that generate a given stiffness had not been individuated. Therefore, we model kinematic performance of nonideal springs to examine force-velocity behavior in the context of the spring's inertia, stiffness, material properties, and geometry.

Spring inertia leads to a force-velocity trade-off for the spring-driven system (Fig. 3), even for the case of the relatively light spring (m_s = 0.1 g) used in the previous section. The net force acting on the projectile depends on position and velocity for both the motor-driven (Fig. 3A) and spring-driven (Fig. 3B) systems, which suggests that force-displacement-velocity trade-offs of springs should be taken into consideration alongside force-velocity trade-offs for motor-driven systems. The force-displacement characteristics of the spring-driven system are set by the spring stiffness, k. Given a fixed maximum force, F_{max}, and range-of-motion, d, for the motor, the spring stiffness determines the amount of elastic energy that the motor can store in the spring. Output of the spring-driven system is therefore sensitive to the stiffness of the spring, which ultimately depends on both the material properties and geometry of the spring.

To illustrate the effect of changing material and geometric properties of the spring, we perform a simulation of the spring-driven system in which the spring is assumed to be a uniform rod, storing and releasing elastic energy under uniaxial compression. The maximum kinetic energy of the spring-driven projectile depends on both cross-sectional area and elastic modulus of the spring material (Fig. 4A) and is strongly dependent on how close the resulting spring stiffness is to the optimal stiffness, k_{opt}. We define k_{opt} as the stiffest spring that can still be loaded a maximum distance d with the same motor. Compared to the $F(x,v)$ relationship for the spring at optimal stiffness (Fig. 3B), using a

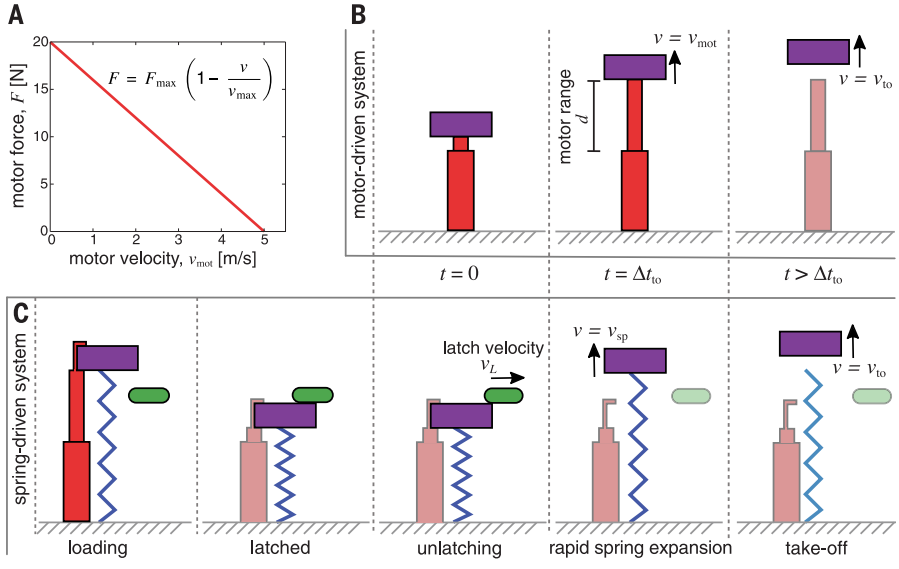

Fig. 1. We mathematically model the factors influencing the power output of a projectile driven by either a motor or a spring. We apply a linear force-velocity trade-off that operates in the same range of force and velocity as a biological motor (muscle) (see Box 1, Glossary, for variable definitions). (**A**) This linear force-velocity trade-off approximates the output of a biological system and exhibits a maximum force (F_{max}) of 20 N and a maximum velocity (v_{max}) of 5 m/s. (**B**) Using the force-velocity relationship in (A), the motor (red) directly launches a projectile (purple) with velocity, v, equal to motor velocity (v_{mot}). At the instant that the projectile leaves the motor, the projectile's velocity is defined as its takeoff velocity (v_{to}). The duration from initiation (t = 0) of projectile movement to its launch is defined as launch duration (Δt_{to}). The projectile's displacement, x, is defined such that $x(t = 0) = 0$. (**C**) The same motor loads a spring (blue) that solely launches the projectile at the velocity of the spring ($v = v_{sp}$). A latch (green) moving at velocity (v_L) controls the timing and release of elastic potential energy.

Box 1. Glossary

σ_y: Yield strength of the spring material.
A: Cross-sectional area of the spring material.
d: Motor range of motion.
E: Young's modulus of spring material.
F(x,v): Force-displacement-velocity relationship. The net force acting on the projectile as a function of its displacement and velocity.
F_{max}: Maximum motor force.
k: Hookean spring constant. Defined by the length, cross-sectional area, and Young's modulus of the spring as $k = EA/L$.
k_{opt}: Optimum Hookean spring constant. Defined by the motor properties as $k_{opt} = F_{max}/d$.
KE: Kinetic energy.
KE_{max}: Maximum kinetic energy reached by the projectile. Defined by the projectile mass and takeoff velocity as $KE_{max} = \frac{1}{2} m v_{to}^2$.
L: Equilibrium length of the spring.
m: Projectile mass.
m_s: Mass of the spring. Defined by the density, length, and cross-sectional area of the spring material as $m_s = \rho LA$.
P_{max}: Maximum power delivered to the projectile during its acceleration.
PA: Power amplification. Defined as the ratio of the maximum power output of the spring-driven to the maximum power output of the motor-driven system driving a given projectile.
PE: Potential energy.
R: Radius of curvature of the latch edge.
SMA: Shape memory alloy.
Δt_{to}: Projectile takeoff duration. Elapsed time from the start of motion until the moment the force acting on the projectile falls to zero.
v: Projectile velocity.
v_L: Velocity at which the latch is removed from blocking the projectile.
v_{max}: Maximum motor velocity.
v_{mot}: Motor velocity.
v_{sp}: Velocity of spring during projectile launch.
v_{to}: Projectile takeoff velocity.
x: Projectile displacement.

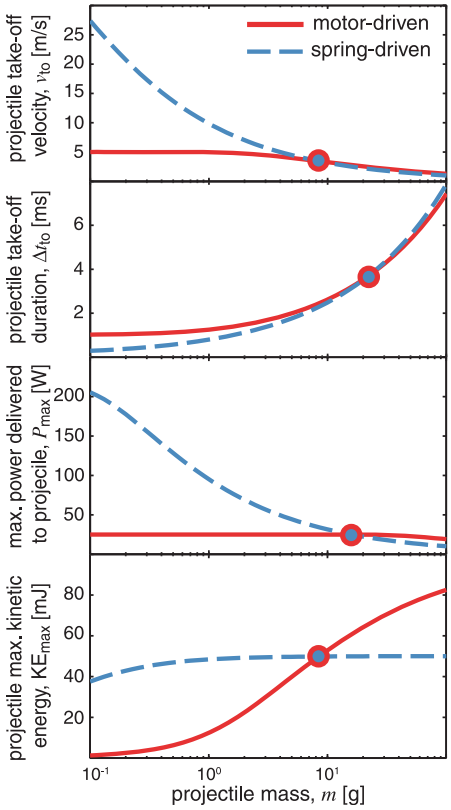

Fig. 2. Projectile launch dynamics diverge in motor-driven versus spring-driven mechanisms when tested across a range of projectiles. Using the models in Fig. 1, we simulate the launch of projectiles of varying mass, m (0.1 to 100 g), and calculate four metrics relevant to the kinematics of projectile launching: takeoff velocity (v_{to}), takeoff duration (Δt_{to}), maximal power output (P_{max}), and maximum kinetic energy (KE_{max}). These performance metrics illuminate key transitions across the projectile sizes. At larger sizes, the motor-driven system performs moderately better than the spring-driven system. At smaller sizes, the spring-driven projectiles experience substantial enhancements in kinetic energy, maximal power, and takeoff velocity compared with motor-driven projectiles.

spring that is either too compliant (Fig. 4B) or too stiff (Fig. 4C) reduces projectile velocity. Stiffness is a composite property that has both geometric and materials contributions. Therefore, if a spring material with a low modulus is used, a larger cross-sectional area of the spring is required to reach k_{opt}. For the same material density, this requires a heavier spring and increases the inertial contribution of the spring, thus reducing the final kinetic energy achieved by the projectile (upper left of Fig. 4A). On the other hand, a spring material with a high modulus requires a small cross-sectional spring area to achieve the optimal stiffness. Small cross-sectional areas lead to high stress and the potential for yielding and failure of the spring material, reducing the kinetic energy of the projectile (lower right of Fig. 4A).

Force-velocity trade-offs therefore guide both motors and springs. Spring-driven motion can be analyzed and synthesized in terms of a net force acting on an inertial load as a function of both its displacement and velocity, $F(x,v)$. Spring power capacity is determined by the inertia of the driven mass, spring materials, and materials failure properties. When the driven mass is much greater than the mass of the spring, the recoil rate of the spring becomes insignificant. On the other hand, springs produce the greatest accelerations while driving the smallest masses, such that spring limitations cannot be ignored. Limits on power amplification depend on how fast springs can recoil and the forces they generate during recoil.

Spring force-velocity behavior may explain spring diversity in biological systems. The small sizes and high accelerations of the most extreme biological systems necessarily constrain the geometries and material properties of their springs. With decreasing size, springs must be proportionally more compliant and geometrically arranged to minimize increasing losses of spring recoil that accompany decreasing size. Varying spring properties in the model would shift the log-log space of Fig. 4A, but the slope would remain consistent. With a more severe force-velocity trade-off at smaller size-scales, the plateau of maximum kinetic energy in Fig. 4A would move toward the material failure regime. This may explain why the larger organisms in Table 1 (e.g., frogs) store energy in long collagen tendons (Young's modulus 0.5 to 1.5 GPa) (*43*, *44*), whereas at smaller scales, energy stores are made out of increasingly stiffer materials. Grasshoppers combine resilin (Young's modulus 1 MPa) and chitinous cuticle (Young's modulus 1 to 40 GPa) to form a composite structure, whereas much smaller froghoppers exclusively use chitinous cuticle, and some plant pollen ejection systems use cellulose (Young's modulus 25 to 150 GPa) (*45*). Few studies have expressly analyzed spring diversity within and across organisms, yet recent analyses point to multiple optima for spring stiffness depending on the temporal limitations set by the animal's behavioral use of the system (*46*).

Using a system repeatedly and repeatably likely involves other material constraints (Table 2). Single-use systems can strain materials to failure, enabling enhanced projection, such as in plant pollen ejection. Likewise, materials available to particular organisms may limit their projection mechanisms. Cellulose, for example, has a much higher Young's modulus than collagen, making cellulose more appropriate to accelerate very small projectiles. Conversely, this may explain why vertebrates, which are limited to using collagen with its far lower Young's modulus, only minimally use elastic structures for direct actuation. By contrast, spring-based actuation is extremely widespread in animals, such as insects, that have chitin in their materials toolbox.

Material and geometric properties of biological springs are diverse (Table 2), yet it is not understood how their architecture influences elastic energy storage capacity, recoil rate, and internal energy dissipation. Arthropod springs are built of multiple materials (*47*–*50*), such as composites of structured stiff, high-energy-density materials bound within softer, resilient matrices (*45*, *51*–*54*). The locust's leg combines the protein resilin with stiff cuticle to generate a flexible yet stiff spring (*48*); resilin provides resilience, while the chitin nanofibers provide the extensional stiffness required for high energy density. Biological springs are typically monolithic, with distributed and integrated flexible and stiff regions. For example, mantis shrimp raptorial appendages dynamically flex both dense, stiff regions and thin, flexible regions during spring loading and release (*55*).

Some engineered springs have been carefully designed to store the maximum amount of energy, given motor or size constraints. They make use of various geometries and materials, including shaped polymer-fiber composites, SMA, molded elastomers, torsional and linear springs, and steel wires and ribbons (Table 2). In one jumping robot, to maximize stored energy density when driven by an electromagnetic motor, a tapered conical cross section of elastomer equalizes shear stress throughout the spring (*56*, *57*). The springs of compound bows and jumping robots (*27*) use specific force-displacement profiles to delay peak acceleration. These systems typically incorporate a nonlinear spring within a more complex mechanism. Some jumping robots use SMA for both actuation and energy storage to reduce size and weight of the integrated system (*32*, *33*), decreasing the inertial component of their force-velocity trade-off.

Experimental analyses of the force-velocity dynamics of springs are needed. Most dynamic materials tests operate at known strain rates and measure resistive force (*58*–*66*). These tests do not reveal how the actual loading and unloading conditions influence recoil dynamics of the spring. Measuring material properties at rates comparable to the natural unloading rate of the spring presents considerable challenges (*67*), yet it is essential to understand how materials properties of springs influence their recoil rate when driving a small mass. Free recoil of rubber and elastic bands have revealed the kinetics of compliant materials with simple geometries (*68*–*74*). Visualization of material deformation for strain rate calculation is viable for these large deformations of compliant materials but difficult in biological springs undergoing small-scale motions at high rates. Measurements of the maximum rates of spring release under variable loading conditions could address questions such as, Which springs convert potential to kinetic energy with minimal internal dissipation? What properties influence recoil time? Does a bending spring recoil faster than one in uniaxial extension?

Dynamics of latch removal

For latches, a short release time yields power amplification, and a sufficiently long duration can completely eliminate power amplification or even result in power attenuation. The central influence of latches in power amplification extends beyond the notion of the latch as a switch or a simple mechanism for energy release. Indeed, latches mediate the time, space, and rate over which potential energy is converted to kinetic energy (Fig. 5A). The latch's force capacity determines the maximum amount of stored energy, given the capacity of the underlying spring. The latch's shape and movement should therefore influence the rate of the spring's delivery of force and velocity to the projectile. Thus, we ask, How do latches mediate the dynamics of energy release? We focus on latches that are simple mechanical structures with adjustable geometry and dynamics.

In this simulation, we incorporate latch removal velocity, shape, force capacity, and mass to determine how these factors influence projectile kinematics. We find that the duration and kinematic profile of latch release are influenced by the latch's shape (Fig. 5B). The latch's shape is altered by increasing the radius of curvature of its edges, which reduces the speed of latch removal and allows the spring to release energy before the latch is fully removed. Consequently, the projectile's kinetic energy declines, the release point shifts (there is more stored energy left in the spring when the latch force goes to zero for a smaller radius latch), and release velocity decreases (constrained by the latch velocity and shape). The projectile's maximum kinetic energy decreases as the latch deviates further from an ideal latch (Fig. 6) in terms of geometry and latch removal kinematics (larger corner radius of curvature and slower latch removal velocity). Latch properties thus dramatically alter the $F(x,v)$ landscape of the spring-driven system (Fig. 6).

Even with many latch designs and patents in engineering, and the diverse evolutionary history of latching and control in biology (Table 2) (*75*, *76*), the relevant metrics and dynamics of latch performance are still in need of basic characterization and analysis. Latches span a range of physical forces, such as osmotic transitions, contact, and phase changes (*76*–*78*) (Tables 1 and 2). Biological latches use contact forces, geometric instability, pressure transitions, and cohesive forces (Table 2). Some trap-jaw ants (Myrmicinae) remove a physical block to release their fast-rotating mandibles (*79*). Venus flytraps use turgor pressure to alter their leaf curvature, such that energy is suddenly released when leaf geometry changes from convex to concave (*80*). Fern sporangia resist energy release with water pressure; sudden cavitation of the water triggers spore release (*17*). Similar in principle to the ferns, snapping shrimp use water cohesion to enable energy storage in the system until sufficient tension is generated and the cohesive forces are overcome (*81*). Ballistospores of the jelly fungus are launched at the instant when two water surfaces coalesce and release surface tension energy (*82*). Grasshoppers use a lever arm system that generates a positive feedback loop to trigger their jumps (*83*).

Latches are necessary for controlling the release of considerable elastic energy over vanishingly short durations. Several kinds of insects—fleas, froghoppers, and leafhoppers—rely on well-tuned relationships between latch linkages and springs to minimize jerk. In these systems, linkages increase mechanical advantage of the spring at approximately the same rate that spring force decreases, resulting in an approximately

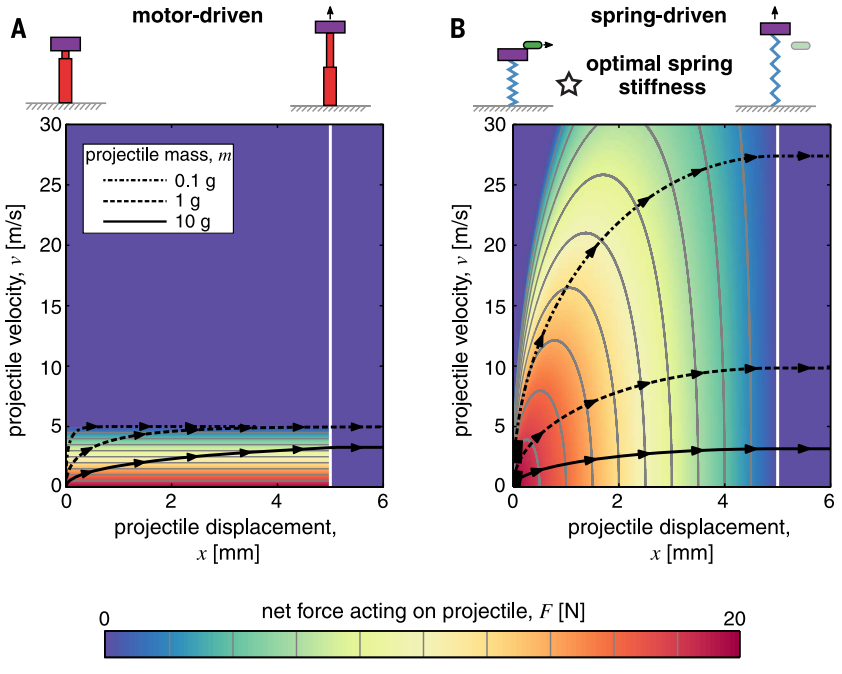

Fig. 3. Motor-driven and spring-driven systems exhibit distinct force-displacement-velocity behavior. Color contours indicate the net force of the motor or spring on the projectile, and black lines depict three examples of different projectile masses with their trajectories through *x*-*v* space (phase space). Takeoff occurs when the projectiles reach the maximum displacement of the motor or spring at $x = d = 5$ mm (vertical white line). (**A**) Motor-driven projectiles, regardless of size, are constrained to takeoff velocities below $v_{max} = 5$ m/s (see motor force-velocity constraints in Fig. 1A). (**B**) Spring-driven projectiles, by contrast, encompass roughly a sixfold greater range of launch velocities than motor-driven projectiles. The spring's force and velocity delivery are determined by a linear, Hookean relationship, but with inertia of the spring included. Therefore, instead of vertical force contour lines in phase space, which would represent a Hookean spring, the force contour lines are curved to reflect the inertial effects of the spring's mass on its force-velocity behavior. The star symbol indicates that optimal spring stiffness is used in the simulation (see Fig. 4) and that the projectile is released using a latch with 0.2 mm radius of curvature (R) and removal velocity (v_L) of 5 m/s (see Fig. 5).

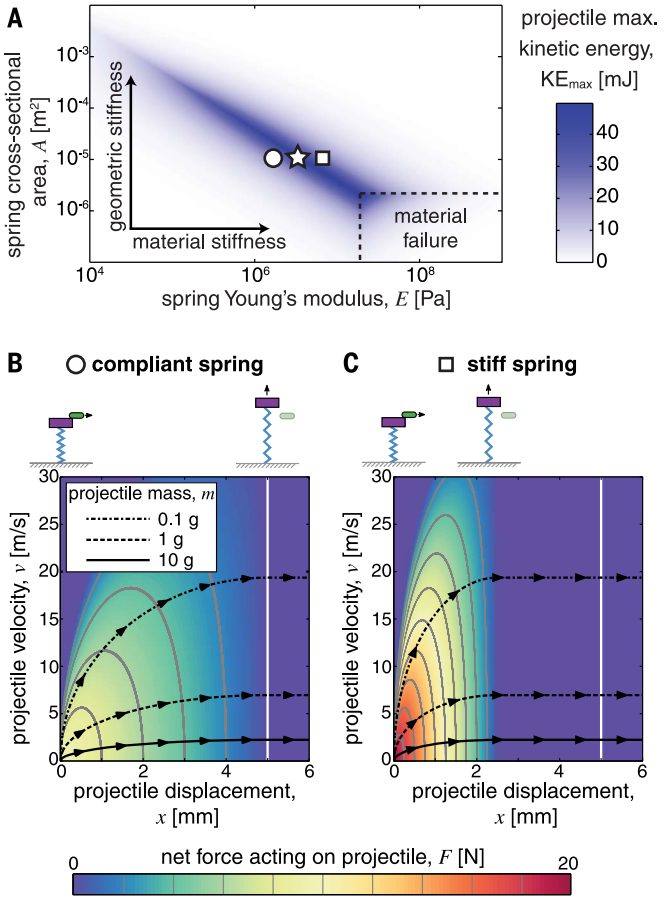

Fig. 4. Spring properties influence the force-velocity profile of projectile launching. (**A**) The spring modulus and cross-sectional area affects the maximum kinetic energy of the projectile (KE$_{max}$). Using the same motor and latch behavior from the previous simulations, the Young's modulus (E) and cross-sectional area (A) of the spring are varied, while keeping a constant spring length (L = 10 mm), density (ρ = 10 kg/m^3), and yield strength (σ_y = 10 MPa). Spring stiffness is calculated as $k = EA/L$. Spring cross-sectional area is a proxy for geometric stiffness. Spring modulus serves as a proxy for material stiffness. Each symbol on the KE$_{max}$ heat map corresponds to the projectile simulations in (B), (C), and Fig. 3. (**B**) A more compliant spring (represented by the circle symbol) yields lower force but similar projectile velocity when compared with (**C**) projectiles launched by a stiffer spring (square symbol). The optimal spring stiffness for achieving maximal projectile velocity is depicted in Fig. 3 (star symbol).

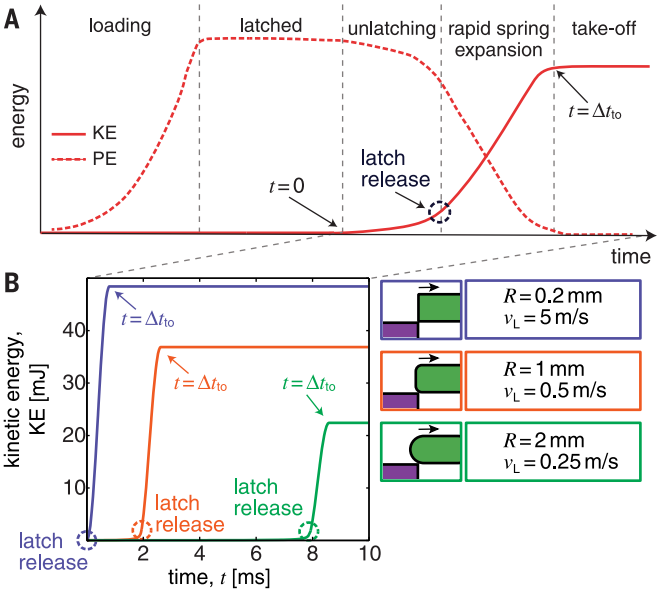

Fig. 5. Latches determine the timing, magnitude and rate of energy release. (**A**) As the spring is loaded, potential energy (PE) (dashed line) in the spring increases. The latch holds the loaded spring in place. Once the latch starts to release, PE decreases and kinetic energy (KE) (solid line) increases until takeoff when the projectile is completely free of the latch. (**B**) Projectile KE is affected by latch shape and rate of removal. Three simulations apply different values for the latch corner radius (R) and latch removal velocity (v_L).

constant acceleration (*49*, *84*). The ability of higher Young's modulus materials to enable energy storage at small scales is likely tied to the origin of latches that are formed through contacting surfaces. Evolutionary origins of latches likely accompanied high-capacity energy storage and the need for tuning of energy release.

Engineered systems also employ a wide variety of latches, including disengagement of physical structures based on contact forces and geometric rearrangements (Table 2). One of the oldest examples of a contact-based force latch is a cam mechanism by Leonardo da Vinci (*85*). This device uses intermittent contact to store potential energy in a slowly rising hammer that generates a large impact when released. The common mousetrap uses a contact latch (physical contact between two structures) that releases the spring-loaded trap upon disengagement (*86*). The small (7 g) jumping robot from Ecole Polytechnique Fédérale de Lausanne (EPFL) is a more modern design that uses the cam mechanism as a contact latch and releases the energy stored in torsional springs; this enables efficient jumping with small payloads through rough terrains (*21*). Inspired by latches in jumping insects, the water strider jumping robot uses a torque reversal catapult (TRC) mechanism to maintain a force profile that enables takeoff on both terrestrial and water surfaces (*32*). A Venus flytrap–inspired system uses bistable composite plates: SMAs slowly push the plates toward an unstable configuration, resulting in a rapid transition between the two stable states (*34*).

Integrated tuning and output of power-amplified systems

Power amplification emerges from the dynamic integration of motors, springs, and latches, yet it has most often been understood as a simple ratio of gross power output relative to power of the underlying motor. In biological systems, it is calculated as the system's power output relative to the maximum power output of the underlying muscle or, in a more conservative approach for systems in which muscle power output has not yet been quantified, relative to the highest measured power output of any biological system. In engineering, power amplification is typically referenced as the enhanced power density of a system. Not only does this approach black-box dynamics of these systems, it also misses the rich array of performance outputs that can be achieved and tuned through integration of these components. Therefore, we ask, What are the general principles of integrated tuning for power-amplified systems?

To achieve the greatest power amplification, spring properties must be optimized and matched to the motor, and the motor's properties must be shifted away from high power output and toward high force output. Spring-driven performance increases with motor force or motor range of motion but does not depend on maximum motor velocity. Therefore, increasing F_{max} or d (even at the expense of v_{max}) improves performance. However, if other elements (e.g., spring or latch) are

fixed, increasing motor force or range of motion does not necessarily lead to improved performance. The system must be fully integrated to confer the benefits of increasing the motor's capabilities.

We mathematically explore integration by allowing the motor's maximum force output to increase (Fig. 7). If spring stiffness is tuned to its optimal value as a function of F_{max}, then maximum kinetic energy of a spring-driven projectile increases monotonically as a function of F_{max} (Fig. 7A, solid blue curve), and power amplification intensifies (Fig. 7B, dashed green curve). On the other hand, if spring stiffness is fixed to the optimal stiffness for F_{max} = 20 N, and, of equal importance, if the motor has no increased range of motion or the position of the latch is fixed, then increasing the motor's maximum force capacity above 20 N does not result in any additional kinetic energy delivered to the projectile (Fig. 7A, dashed red curve), and power amplification is diminished for F_{max} = 30 N (Fig. 7B, dash-dotted orange curve). In other words, although a motor with a larger force capacity has the potential capability to produce more energy, unless the spring can store that energy over the limited range of motion of the motor, the motor will not reach its maximum force capacity and the overall performance of the system will not improve. This coupling is important not only between the spring and motor but also between all elements of the system, including the latch.

Even though the model is composed of few components, defined in the simplest terms, and with a modest array of nonideal behaviors, the outputs venture into a richer space than expected from previous research. Integration of these components not only determines the array of outputs and transition points, it also enables analysis of failure and scaling limits as more parameters are incorporated. A particular strength of power-amplified systems, especially ones with spring actuation, is that components are often spatially and temporally separated and thereby enable a modular approach to both synthesis and analysis.

When our modeling results are placed in the context of the diversity of biological systems and the limited array of engineered systems, it is clear that integration is central to achieving a rich performance space. The components of biological systems necessarily evolved together, yet engineering design often struggles to achieve similarly tuned integration. Only a few studies and systems have been examined in the context of tuning and integration to achieve power amplification. The mantis shrimp's motor, spring, and projectile coevolved as integrated components (*87*–*91*), such that species producing the greatest accelerations evolved springs with greater work capacity and muscles with force-modified architecture at the expense of contraction velocity. They evolved with varying degrees of integration (i.e., correlated change among components): More tightly integrated components are associated with greater acceleration and spring work but with slower accumulation of change over evolutionary time (*89*). This trade-off between integration and evolvability is relevant to engineering design, given that retaining flexibility or modularity of design for different goals may bear a cost in terms of integration and performance.

Integrated design approaches offer a key pathway for achieving improved dynamics and scaling in engineered systems. The tuning of engineered jumpers has been examined, including a galago-inspired jumping robot (*56*). In this case, various configurations of motors, springs, and linkages were compared using a vertical jumping agility metric (a combination of jump height and frequency). With the motor and spring in series, which enabled rapid leg repositioning for multiple jumps, a linkage was used to modulate the power delivery from the spring to the ground. Even though the spring was not included in this particular optimization [other studies have incorporated spring optimization analyses; see (*57*, *92*)], the galago study analyzed trade-offs between motor power density and linkage design for series elastic jumpers. Navigation of the rich design space for engineered systems may be particularly challenging; however, advances in additive manufacturing alleviate this challenge,

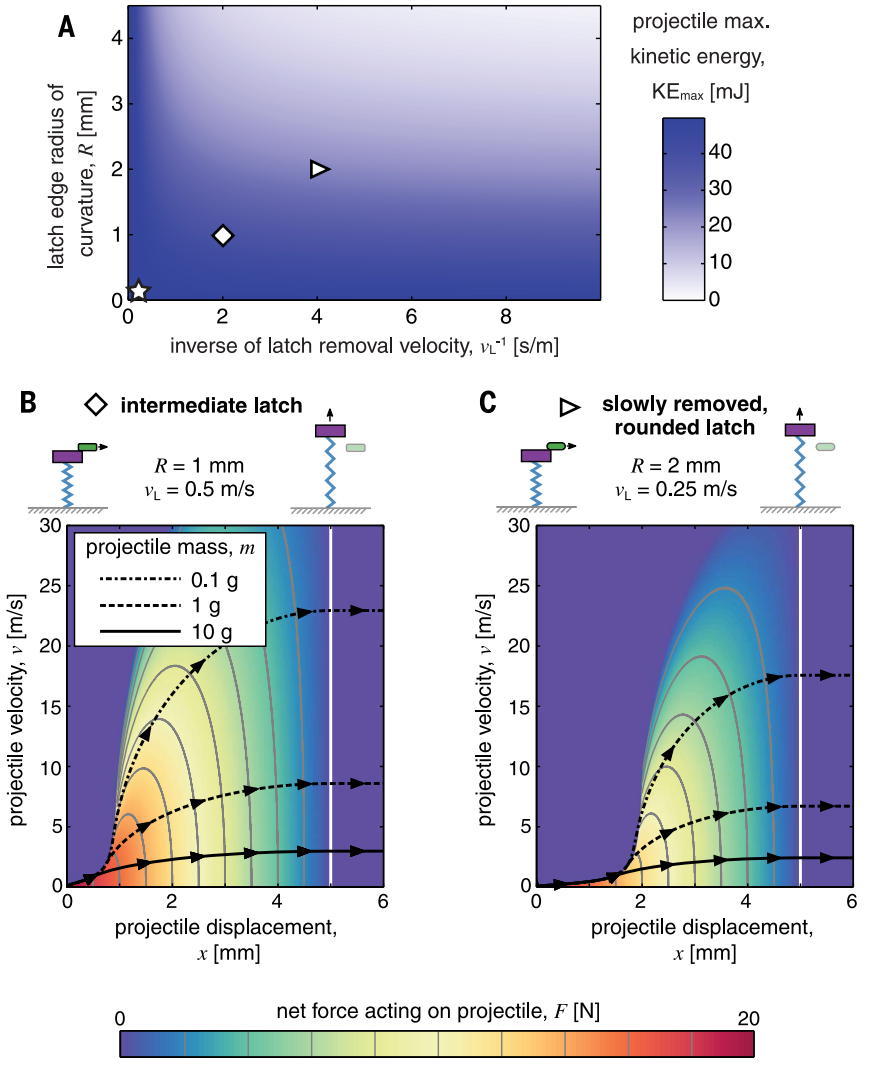

Fig. 6. Latch geometry and latch removal kinematics influence projectile kinetic energy and the force-velocity profile of spring-driven launches. (**A**) The maximum kinetic energy of the projectile (KE$_{max}$) decreases as the latch's radius of curvature (R) (see Fig. 5) is increased (star, R = 0.2 mm; diamond, R = 1 mm; triangle, R = 2 mm) and latch removal speed (v_L) is decreased (increased inverse latch removal speed, $1/v_L$). The star symbol refers to the simulation depicted in Fig. 3B, to which both optimal latch and spring dynamics were applied. (**B**) This simulation applied the 1 mm radius of curvature latch at 0.5 m/s latch removal speed (diamond). In this case, force on the projectile was preserved and launch velocity remained high for small projectiles. (**C**) Incorporation of a large radius of curvature (2 mm) and slower removal velocity (0.25 m/s) caused a substantial reduction in force development during launching, which primarily affected the kinematics of smaller projectiles.

where, as in self-assembly, the cost of complexity is dramatically reduced (*93*).

Applications

A natural next question is whether this model can be applied to even broader challenges, such as establishing design principles underlying biological diversity. Scaling of power-amplified biological systems has generated centuries of hypotheses from Borelli to Vogel (*94*). The most widely accepted scaling explanation is that jump performance (kinetic energy) scales with body mass and muscle volume. However, as pointed out by Vogel (*95*, *96*), this scaling pattern persists in organisms that lack muscles, implying that muscle-volumetric scaling is not sufficient to explain enhanced performance at small sizes and declining performance at larger sizes. Our findings suggest a more complete explanation for the scaling of power-amplified systems in biology that incorporates a lower size limit, an upper size limit, and an approach to addressing "optimal" size (Fig. 8).

The upper size limit of biological power-amplified systems has garnered the most attention: Why are power-amplified systems exclusively small (Fig. 8A)? Our analysis of muscle-spring dynamics answers that question (Fig. 2): Above a certain size, a spring does not enhance kinematic output and an organism is best served by using muscle. However, the inverse question is rarely asked: Why does kinematic performance fall off at smaller sizes in jumping insects (Fig. 8B)? Our analysis suggests that a trade-off between Young's modulus and size may reduce performance at smaller scales (Fig. 4A). To actuate motion with a spring and achieve high performance at small scales, the Young's modulus must be large. However, as Young's modulus increases and spring cross-sectional area decreases, the failure limit of the material will be reached and thereby sets a lower size limit to spring actuation.

Upper and lower limits to muscle-based power amplification may explain a conundrum in the scaling of jumping insects: The smallest insects and the largest insects jump more slowly than midsized insects (Fig. 8B). Fleas (0.5-mg body mass) have a low takeoff velocity relative to other spring-loaded jumpers (*97*, *98*), whereas the best-recorded jumpers have body mass on the order of 10s of milligrams [e.g., froghoppers: 5 to 6 m/s, 20 to 50 mg (*99*); pygmy mole crickets: 5 to 6 m/s, 10 mg (*98*, *100*)]. Given the constraints of their materials toolbox, and following the inherent trade-off between Young's modulus and cross-sectional area (Fig. 4A), insect springs are also likely to decrease in performance with decreasing size. In other words, at a threshold

Table 1. Fast biological systems are used for a greater diversity of functions and operate at smaller size scales than engineered systems. Kinematics of a representative sample of fast biological and engineered movements are arranged by characteristic length scale. Characteristic length represents projectile length (e.g., stinging needle of nematocysts and magnet from chameleon coil gun), accelerated part length (e.g., combustion-based jumping systems, jumping insects, and mandibles of trap-jaw ants), or the leg length for jumping robots, given that legs are the dominant length in these systems. Duration represents acceleration time. Distance represents maximum horizontal or vertical distance traveled by a projectile, jumping system, or maximum rotation of striking and trapping systems. Biological movements operate in air (frog, grasshopper, Venus flytrap, trap-jaw ant, fungi, and chameleon) or water (mantis shrimp, *Hydra*, and bladderworts). All listed engineered systems are designed for operation in air, although the water strider robot jumps at the air-water interface. Char., characteristic; Max., maximum; Accel., acceleration. *Estimated or calculated values from figures or data reported. **Velocity and acceleration of fluid displaced by bladderwort trap.

Movement	System	Char. length (m)	Mass (kg)	Duration (s)	Distance (m)	Max. speed (m/s)	Accel. (m/s^2)	References
Biological systems								
Nematocyst discharge	*Hydra*	2.4×10^{-5}*	2.3×10^{-12}	1×10^{-6}*	1.3×10^{-5}	3.7×10^{1}	5.4×10^{7}	(*103*, *106*)
Ballistospore ejection	Fungi	4.2×10^{-6}	3.7×10^{-13}*	1×10^{-5}*	4.0×10^{-4}*	1.6	1.2×10^{5}	(*107*)
Pollen ejection	Bunchberry dogwood stamen	8.0×10^{-4}	4.0×10^{-7}	4.0×10^{-4}	1.2×10^{-3}	7.5	2.4×10^{4}	(*108*, *109*)
Mandible strike	Trap-jaw ant	1.4×10^{-3}	1.5×10^{-7}	6×10^{-5}	–	6.4×10^{1}	1×10^{6}	(*110*)
Jump	Plant louse	1.9×10^{-3}	7.0×10^{-7}	4×10^{-4}	1.5×10^{-3}	2.5	6.3×10^{3}	(*111*)
Suction trap	Aquatic bladderworts	2.0×10^{-3}	–	1×10^{-3}	–	1.5**	6.0×10^{3}**	(*18*)
Jump	Froghopper	6.1×10^{-3}	1.2×10^{-5}	8.8×10^{-4}	7.0×10^{-1}	4.7	5.4×10^{3}	(*99*)
Snap buckling	Venus flytrap	1.0×10^{-2}	–	1.0×10^{-1}	–	1.0×10^{-2}	–	(*20*)
Appendage strike	Mantis shrimp	8.2×10^{-3}	9.2×10^{-3}	2.7×10^{-4}	–	3.1×10^{1}	2.5×10^{5}	(*112*)
Jump	Frog	4.1×10^{-2}	8.8×10^{-3}	5.4×10^{-2}	2.2	4.5	1.4×10^{2}	(*113*)
Tongue projection	Chameleon	2.0×10^{-2}*	8.7×10^{-5}	6×10^{-3}*	1.2×10^{-1}	5.3	2.6×10^{3}	(*114*, *115*)
Jump	Locust	5.0×10^{-2}	1.8×10^{-3}	3×10^{-2}*	9.5×10^{-1}	3.2	1.8×10^{2}	(*116*)
Engineered systems								
Jump	Micro elastomer jumper	4.0×10^{-3}	8.0×10^{-6}	–	3.2×10^{-1}	3.0	–	(*117*)
Jump	Energetic silicon jumper	7.0×10^{-3}	3.1×10^{-4}	–	8.0×10^{-2}	1.3	–	(*37*)
Projection	Chameleon tongue–inspired sys.	8.0×10^{-3}	7.7×10^{-4}	8.0×10^{-3}	1.6×10^{-1}	5.4	9.2×10^{2}	(*118*)
Jump	Flea-inspired robot	3.0×10^{-2}	2.3×10^{-3}	8.0×10^{-3}	1.2	7.0	8.8×10^{2}*	(*119*)
Jump	Steerable MSU jumper	3.3×10^{-2}	2.4×10^{-2}	–	9.0×10^{-1}	4.3	-	(*120*)
Jump	Water strider–inspired robot	5.0×10^{-2}	6.8×10^{-5}	2×10^{-2}*	1.4×10^{-1}	1.6	1.4×10^{2}	(*32*)
Jump	EPFL 7 g robot	5.0×10^{-2}*	7.0×10^{-3}	1.5×10^{-2}	1.4	6.0	4.0×10^{2}*	(*21*)
Jump	JPL hopper (2nd gen.)	1.0×10^{-1}*	1.3	–	2.0	–	–	(*27*)
Strike, catch	High-speed fingered hand	1.1×10^{-1}	1.0×10^{-1}*	2×10^{-2}	180°	4.5	2×10^{2}*	(*30*)
Jump	Locust-inspired robot	1.4×10^{-1}	2.3×10^{-2}	2×10^{-2}	3.7	9.0	4×10^{2}*	(*31*)
Catch	Flytrap-inspired robot	1.5×10^{-1}	–	4.1×10^{-1}	90°	–	–	(*34*)
Jump	Galago-inspired "Salto" robot	1.5×10^{-1}	1.0×10^{-1}	–	1.0	–	–	(*56*)
Jump	Sand flea–inspired robot	1.5×10^{-1}	5.0	–	1.0×10^{1}	–	–	(*39*)
Jump	Sandia Mars hopper	2.0×10^{-1}*	5.0×10^{-1}	–	1.8	–	–	(*121*, *122*)
Jump	Soft combustion robot	3.0×10^{-1}*	9.7×10^{-1}	–	7.6×10^{-1}	–	–	(*93*)
Jump	Bipedal jumper "Mowgli"	6.0×10^{-1}*	3.0	2.5×10^{-1}	5.0×10^{-1}	–	–	(*38*)

specific to their elastic system, the smallest jumpers cannot load their springs without encountering failure. Other biological systems at the scale of fleas that achieve greater kinematic performance should therefore be using either different materials (i.e., cellulose) or different mechanisms that circumvent material limits at small scales. (e.g., the surface tension catapult of fungal ballistospores).

Our simple model can be parameterized to pinpoint limits and optima that are system-specific and can be extended to engineered systems. Performance limits and optimal mass have been found for small engineered jumpers based on environmental drag; similar methods can be extended to motor-spring dynamics and material limits (*101*). Even so, compared to the impressive diversity of motion and scales in biological systems (which are naturally fully inclusive of power, control, and actuation), engineered systems occupy a relatively narrow range of dynamics, scales, and uses (Table 2 and Fig. 8A) (*35*, *36*), and our analyses suggest a far broader range of potential capabilities for synthetic systems.

Limitations

By adjusting the scaling of our archery example, the multifaceted challenges of energy dissipation become apparent. Energy dissipation begins with heat produced by the actively contracting arm muscles and continues through material dissipation of the contracting and releasing spring, frictional or hysteresis losses of the latching mechanism, and interaction between the arrow, gravity, and its fluid environment while moving toward its target. The environment surrounding the arm and bow necessarily influences the amount of dissipation, especially in the context of scaling. For an arrow flying through air at high Reynolds numbers [Re, a dimensionless measure of the relative importance of inertial and viscous forces in a flow (*102*)], drag forces scale with the second power of the arrow velocity and cause external dissipation. However, if the arrow is scaled down to the size of many small power-amplified systems, drag forces increase linearly with velocity (low Re limit), thus changing the scaling of the external dissipation (*102*).

If we move the elastic bow from air to liquid—the internal environment of most biological springs—dissipation increases substantially. Small Re is relevant for microscale systems, such as the puncturing needles of nematocysts (*103*): Projectile dynamics are dominated by viscous effects, inertia is of no consequence, and the dynamics are counterintuitive (*104*). Additional complexity occurs when the ambient fluid is non-Newtonian or complex [i.e., not characterized by a single, constant parameter such as viscosity (*105*)]. The rheology of the materials constituting the spring and latch can assume greater importance at small scales. Our

Table 2. Fast movement is achieved through integration of diverse motor, spring, and latch components, with some systems operating repeatedly and others self-destructing after one use. Repeatable systems (R) function many times, whereas single-shot systems operate only once (NR). Latch mechanisms include contact (physical contact between two structures), fluidic (mediated by microscopic and macroscopic fluid properties), and geometric (dependent on changes in forces, moment arms, and elastic instabilities due to geometrical configurations). A final distinction is whether the system can repeat the motion without external manipulations (R-i) or external manipulation is required to prepare the system to fire again (R-e). Any repeatable biological system must be able to internally reset the system. However, many engineered systems still require an external device (or person) to reconfigure the system to the correct condition to fire again. DC, direct current; MA, mechanical advantage; SMA, shape memory alloy; TRC, torque reversal catapult; Repeat., repeatability.

Movement	System	Work input	Energy storage	Latch	Repeat.	References
Biological systems						
Appendage strike	Mantis shrimp	Muscle contraction	Exoskeleton	Contact	R-i	(*123*)
Claw closure	Snapping shrimp	Muscle contraction	Exoskeleton	Fluidic (cohesion)	R-i	(*81*, *124*)
Jump	Frog	Muscle contraction	Plantaris tendon	Geometric	R-i	(*125*, *126*)
Jump	Grasshoppers, locusts	Muscle contraction	Resilin and chitin	Geometric	R-i	(*47*, *48*)
Leaf closure	Venus flytrap	Turgor pressure	Cell wall	Geometric (instability)	R-i	(*20*)
Mandible closure	Trap-jaw ant	Muscle contraction	Exoskeleton	Contact	R-i	(*79*, *110*)
Nematocyst discharge	*Hydra*	Osmotic gradient	Cell membrane	Cohesion	NR	(*103*)
Spore ejection	Basidiomycota fungi	Water condensation	Surface tension	Fluidic (coalescence)	NR	(*107*, *127*)
Spore ejection	Fern sporangium	Dehydration	Annulus wall	Fluidic (pressure)	NR	(*17*)
Stalk contraction	Vorticella	Ionic gradient	Spasmoneme protein	Unknown	R-i	(*128*)
Tongue projection	Chameleon	Muscle contraction	Collagen sheaths	Contact	R-i	(*129*, *130*)
Water suction	Bladderworts	Osmotic gradient	Trap wall	Geometric (instability)	R-i	(*18*)
Engineered systems						
Catch	Flytrap-inspired robot	SMA contraction	Bistable composite	Geometric (instability)	R-i	(*34*)
Jump	Micro elastomer jumper	External force	Elastomer tension	Contact	R-e	(*117*)
Jump	EPFL 7 g robot	DC motor	Steel torsion	Contact	R-i	(*21*)
Jump	Steerable MSU jumper	DC motor	Steel torsion	Geometric	R-i	(*120*)
Jump	JPL hopper (2nd gen.)	DC motor	Steel torsion	Contact	R-i	(*27*)
Jump	Locust-inspired robot	DC motor	Steel torsion	Contact	R-i	(*31*)
Jump	Galago-inspired "Salto" robot	DC motor	Elastomer torsion	Geometric (MA)	R-i	(*56*)
Jump	Water strider–inspired robot	SMA contraction	SMA sheet + cantilever	Geometric (TRC)	R-e	(*32*)
Jump	Flea-inspired robot	SMA contraction	SMA coil	Geometric (TRC)	R-e	(*119*)
Jump	Energetic silicon jumper	Directly powered by chemical reaction			NR	(*37*)
Jump	Soft combustion robot	Directly powered by chemical reaction			R-e	(*93*)
Jump	Sandia Mars hopper	Directly powered by chemical reaction			R-i	(*121*, *122*)
Jump	Bipedal jumper "Mowgli"	Directly powered by pneumatic actuation			R-i	(*38*)
Projection	Chameleon tongue–inspired sys.	Directly powered by electromagnetic coilgun			R-i	(*118*)
Strike	Mousetrap	External force	Steel torsion	Contact	R-e	(*86*)
Strike, catch	High-speed fingered hand	Directly powered by DC motor			R-i	(*30*)

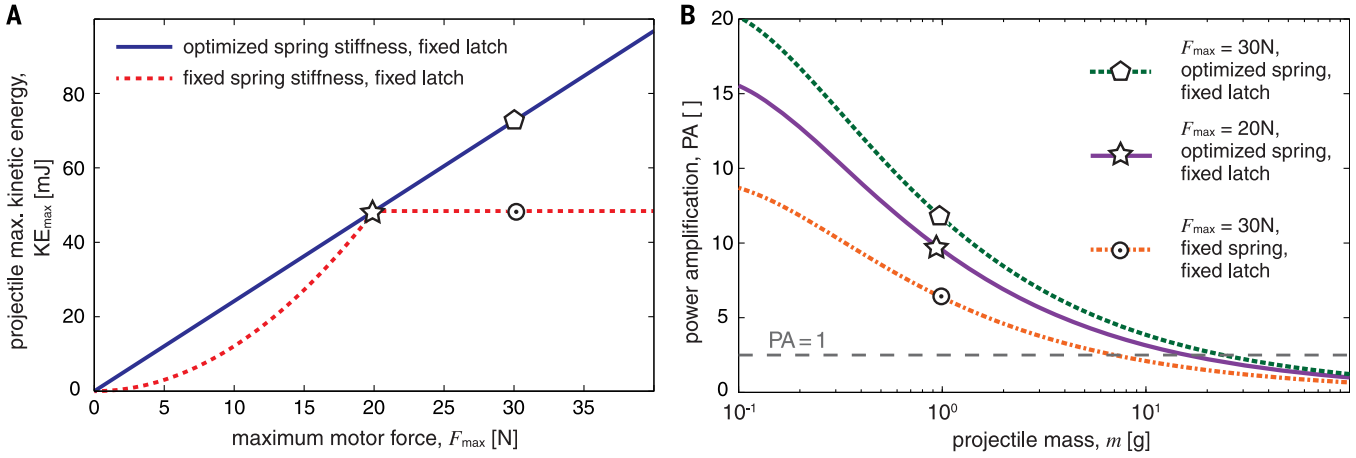

Fig. 7. Power amplification and kinetic energy represent the effects of strategic tuning of springs, motors, and latches. (**A**) The dependence of the maximum kinetic energy of a projectile on the motor force capacity is determined by whether the spring stiffness is optimized as a function of motor force (blue solid curve) or is fixed (red dashed curve). This simulation is applied to a m = 1 g projectile. We simulate a motor with expanded force capacity compared with previous simulations (Fig. 1A), while keeping the motor range of motion fixed. Spring properties are optimized using the process illustrated in Fig. 4A. (**B**) Power amplification, PA (the ratio of maximum power delivered to the projectile from the spring-driven or motor-driven system), is strongly influenced by both the tuning of spring properties to motor properties and the projectile mass, particularly at smaller sizes. We simulate power amplification using earlier spring configurations (A) and again increase the force capacity of the motor. Tuning spring properties to motor force capacity enhances power amplification beyond what is achieved with a fixed spring stiffness, exemplifying the need to integrate and tune the motor, spring, and projectile load when attempting to maximize the projectile kinematics.

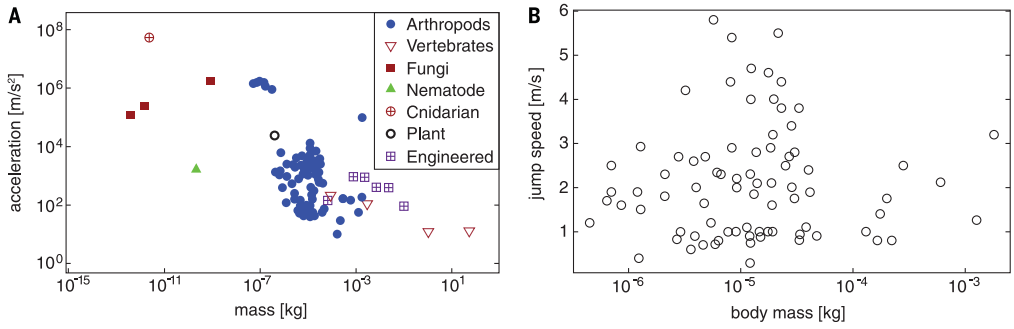

Fig. 8. Power-amplified biological systems span orders of magnitude in acceleration and mass, yet smaller sizes may not always confer benefits in terms of speed. (**A**) The most extreme accelerations are found in fungi and the stinging cells of cnidarians, whereas the top accelerations in the arthropods are performed by trap-jaw ants and mantis shrimp. Engineered systems exceed some vertebrates but have yet to extend into the dynamics and mass scales of most power-amplified biological systems. (**B**) Even though broad comparisons of acceleration and mass demonstrate increasing acceleration at smaller masses, a closer look at the jumping velocities of insects reveals peak jumping speeds at an intermediate size. Engineering data are from Table 1. Biological data are listed in table S3.

mathematical model can be improved by including environment-system interactions and incorporating a more detailed analysis of the friction and mechanical interactions during unlatching. In addition, the role of time-dependent viscoelastic materials, which are ubiquitous in nature and engineering, should be incorporated into the motor, spring, and latch. Extension of our current framework to include dissipative elements will further illuminate design principles that very small-scale power-amplification systems encounter and successfully resolve.

Conclusions

Our results explore and resolve the intriguing intersection of force-velocity dynamics, size, and materials in the diversity and performance of biological and engineered power amplification. We discovered that $F(x,v)$ of a spring-driven system is a whole-system property of the combined motor, spring, latch, and projectile. As demonstrated through a parameterized latch model, latch design has a substantial impact on performance. Optimal spring design requires careful tuning of spring stiffness to motor properties, which can be achieved through geometric or materials stiffness. Ultimately, the spring's stiffness combined with its force-velocity trade-off and material failure properties set an optimal size-scale of the spring: A large spring is slowed down by its own force-velocity trade-off, whereas a small spring is more likely to fail. Individual components of power-amplified systems and their interactions are essential to dynamic outputs and offer a greater potential for kinematic performance than has been previously recognized.

This study demonstrates the rich potential for understanding, analyzing, and designing effective, integrated dynamics of power-amplified systems. Analysis of power-amplified systems provides an important opportunity to establish fundamental principles of actuators, materials, and latches in their own right and in the context of their dynamic interactions. Researchers across the fields of mathematics, engineering, and biology are well poised to resolve these new and classic challenges through advances in high-speed imaging, materials testing and synthesis, integrated engineering design systems, and new biological discoveries.

Methods

The comparative biological data set was constructed based on an exhaustive literature search of fast movements in biology. This initial data set

consisted of 278 species-level data points about fast organismal movement. This data set was then reduced to include only species for which the mass of the accelerated component was reported and then reduced again to include only one entry per species, such that the final data set of 104 species was compiled from the most recent or most high-quality kinematic data set. When available, the maximum reported acceleration and velocity were included in the data set and, if a range was not provided, we instead included the average reported values. If maximum acceleration and average acceleration were not reported, acceleration was estimated from the ratio of maximum speed to duration in Table 1.

A mathematical model was constructed using a linear elastic spring and a geometric latch model described in the supplementary text (along with tables S1 and S2 and figs. S1 to S12). For a given set of motor, spring, latch, and load mass parameters, the latch release time was numerically calculated using MATLAB. From the latch release time, the kinematic variables (force-displacement-velocity relationship, takeoff velocity, maximum power, projectile takeoff duration, and maximum kinetic energy) were calculated using the equations in sections S1 to S6 of the supplementary materials.

REFERENCES AND NOTES

1. P. Aerts, Vertical jumping in *Galago senegalensis*: The quest for an obligate mechanical power amplifier. *Philos. Trans. R. Soc. Lond. B Biol. Sci.* **353**, 1607–1620 (1998). doi: 10.1098/rstb.1998.0313
2. M. M. Peplowski, R. L. Marsh, Work and power output in the hindlimb muscles of Cuban tree frogs *Osteopilus septentrionalis* during jumping. *J. Exp. Biol.* **200**, 2861–2870 (1997). pmid: 9344973
3. M. Burrows, Biomechanics: Froghopper insects leap to new heights. *Nature* **424**, 509 (2003). doi: 10.1038/424509a; pmid: 12891345
4. O. Barth, Harmonic piezodrive—miniaturized servo motor. *Mechatronics* **10**, 545–554 (2000). doi: 10.1016/S0957-4158(99)00062-8
5. L. C. Rome, S. L. Lindstedt, The quest for speed: Muscles built for high-frequency contractions. *Physiology* **13**, 261–268 (1998). doi: 10.1152/physiologyonline.1998.13.6.261; pmid: 11390801
6. T. J. Roberts, E. Azizi, Flexible mechanisms: The diverse roles of biological springs in vertebrate movement. *J. Exp. Biol.* **214**, 353–361 (2011). doi: 10.1242/jeb.038588; pmid: 21228194
7. S. N. Patek, D. M. Dudek, M. V. Rosario, From bouncy legs to poisoned arrows: Elastic movements in invertebrates. *J. Exp. Biol.* **214**, 1973–1980 (2011). doi: 10.1242/jeb.038596; pmid: 21613512
8. W. Gronenberg, Fast actions in small animals: Springs and click mechanisms. *J. Comp. Physiol. A Neuroethol. Sens. Neural Behav. Physiol.* **178**, 727–734 (1996). doi: 10.1007/BF00225821
9. R. McN. Alexander, H. C. Bennet-Clark, Storage of elastic strain energy in muscle and other tissues. *Nature* **265**, 114–117 (1977). doi: 10.1038/265114a0; pmid: 834252
10. R. M. Alexander, *Elastic Mechanisms in Animal Movement* (Cambridge Univ. Press, 1988).
11. D. P. Ferris, M. Louie, C. T. Farley, Running in the real world: Adjusting leg stiffness for different surfaces. *Proc. R. Soc. London Ser. B* **265**, 989–994 (1998). doi: 10.1098/rspb.1998.0388; pmid: 9675909
12. A. Galantis, R. C. Woledge, The theoretical limits to the power output of a muscle-tendon complex with inertial and gravitational loads. *Proc. R. Soc. London Ser. B* **270**, 1493–1498 (2003). doi: 10.1098/rspb.2003.2403; pmid: 12965015
13. S. N. Patek, The most powerful movements in biology. *Am. Sci.* **103**, 330–337 (2015). doi: 10.1511/2015.116.330
14. D. Cofer, G. Cymbalyuk, W. J. Heitler, D. H. Edwards, Neuromechanical simulation of the locust jump. *J. Exp. Biol.* **213**, 1060–1068 (2010). doi: 10.1242/jeb.034678; pmid: 20228342
15. W. Gronenberg, B. Ehmer, The mandible mechanism of the ant genus *Anochetus* (Hymenoptera, Formicidae) and the possible evolution of trap-jaws. *Zoology* **99**, 153–162 (1996).
16. M. M. Blanco, S. N. Patek, Muscle trade-offs in a power-amplified prey capture system. *Evolution* **68**, 1399–1414 (2014). doi: 10.1111/evo.12365; pmid: 24475749
17. X. Noblin *et al.*, The fern sporangium: A unique catapult. *Science* **335**, 1322 (2012). doi: 10.1126/science.1215985; pmid: 22422975
18. O. Vincent *et al.*, Ultra-fast underwater suction traps. *Proc. R. Soc. London Ser. B* **278**, 2909–2914 (2011). doi: 10.1098/rspb.2010.2292; pmid: 21325323
19. J. M. Skotheim, L. Mahadevan, Physical limits and design principles for plant and fungal movements. *Science* **308**, 1308–1310 (2005). doi: 10.1126/science.1107976; pmid: 15919993
20. Y. Forterre, J. M. Skotheim, J. Dumais, L. Mahadevan, How the Venus flytrap snaps. *Nature* **433**, 421–425 (2005). doi: 10.1038/nature03185; pmid: 15674293
21. M. Kovac, M. Fuchs, A. Guignard, J.-C. Zufferey, D. Floreano, *in IEEE International Conference on Robotics and Automation* (IEEE, 2008), pp. 373–378.
22. F. Li *et al.*, Jumping like an insect: Design and dynamic optimization of a jumping mini robot based on bio-mimetic inspiration. *Mechatronics* **22**, 167–176 (2012). doi: 10.1016/j.mechatronics.2012.01.001
23. J. Zhao, in *IEEE International Conference on Robotics and Automation* (IEEE, 2011), pp. 4614–4619.
24. B. G. A. Lambrecht, A. D. Horchler, R. D. Quinn, in *IEEE International Conference on Robotics and Automation* (IEEE, 2005), pp. 1240–1245.
25. S. A. Stoeter, P. E. Rybski, M. Gini, N. Papanikolopoulos, in *IEEE Int. Conf. Intell. Robot. Syst.* **1**, 721–726 (2002).
26. N. Fukamachi, H. Mochiyama, in *IEEE International Conference on Advanced Intelligent Mechatronics* (IEEE, 2015) pp. 1102–1107.
27. J. Burdick, P. Fiorini, Minimalist jumping robots for celestial exploration. *Int. J. Robot. Res.* **22**, 653–674 (2003). doi: 10.1177/02783649030227013
28. M. Kaneko, M. Higashimori, in *Automation Congress* (IEEE, 2004), pp. 117–122.
29. A. M. Johnson, D. E. Koditschek, in *IEEE International Conference on Robotics and Automation* (IEEE, 2013), pp. 2568–2575.
30. A. Namiki, Y. Imai, M. Ishikawa, M. Kaneko, in *IEEE/RSJ International Conference on Intelligent Robots and Systems* (IEEE, 2003), pp. 2666–2671.
31. V. Zaitsev *et al.*, A locust-inspired miniature jumping robot. *Bioinspir. Biomim.* **10**, 066012 (2015). doi: 10.1088/1748-3190/10/6/066012; pmid: 26602094
32. J. S. Koh *et al.*, Jumping on water: Surface tension-dominated jumping of water striders and robotic insects. *Science* **349**, 517–521 (2015). doi: 10.1126/science.aab1637; pmid: 26228144
33. J. S. Koh, S. Jung, R. J. Wood, K. Cho, in *IEEE/RSJ International Conference on Intelligent Robots and Systems* (IEEE, 2013), pp. 3796–3801.
34. S. W. Kim *et al.*, Flytrap-inspired robot using structurally integrated actuation based on bistability and a developable surface. *Bioinspir. Biomim.* **9**, 036004 (2014). doi: 10.1088/1748-3182/9/3/036004; pmid: 24615620
35. W. Lindsay, D. Teasdale, V. Milanovic, K. Pister, C. Fernandez-Pello, in *IEEE International Conference on Micro Electro Mechanical Systems* (IEEE, 2001), pp. 606–610.
36. S. J. Apperson *et al.*, Characterization of nanothermite material for solid-fuel microthruster applications. *J. Propuls. Power* **25**, 1086–1091 (2009). doi: 10.2514/1.43206
37. W. A. Churaman, L. J. Currano, C. J. Morris, J. E. Rajkowski, S. Bergbreiter, The first launch of an autonomous thrust-driven microrobot using nanoporous energetic silicon. *J. Microelectromech. Syst.* **21**, 198–205 (2012). doi: 10.1109/JMEMS.2011.2174414
38. R. Niiyama, A. Nagakubo, in *IEEE International Conference on Robotics and Automation* (IEEE, 2007), pp. 2546–2551.
39. Boston dynamics Inc., Sandflea, https://www.bostondynamics.com/sandflea.
40. H. Tsukagoshi, M. Sasaki, A. Kitagawa, T. Tanaka, in *IEEE International Conference on Robotics and Automation* (IEEE, 2005), pp. 1276–1283.
41. F. E. Zajac, Muscle and tendon: Properties, models, scaling, and application to biomechanics and motor control. *Crit. Rev. Biomed. Eng.* **17**, 359–411 (1989). pmid: 2676342
42. T. J. Roberts, R. L. Marsh, Probing the limits to muscle-powered accelerations: Lessons from jumping bullfrogs. *J. Exp. Biol.* **206**, 2567–2580 (2003). doi: 10.1242/jeb.00452; pmid: 12819264
43. R. F. Ker, Dynamic tensile properties of the plantaris tendon of sheep (*Ovis aries*). *J. Exp. Biol.* **93**, 283–302 (1981). pmid: 7288354
44. R. F. Ker, R. McN. Alexander, M. B. Bennett, Why are mammalian tendons so thick? *J. Zool.* **216**, 309–324 (1988). doi: 10.1111/j.1469-7998.1988.tb02432.x
45. J. F. V. Vincent, U. G. K. Wegst, Design and mechanical properties of insect cuticle. *Arthropod Struct. Dev.* **33**, 187–199 (2004). doi: 10.1016/j.asd.2004.05.006; pmid: 18089034
46. M. V. Rosario, G. P. Sutton, S. N. Patek, G. S. Sawicki, Muscle-spring dynamics in time-limited, elastic movements. *Proc. R. Soc. London Ser. B* **283**, 20161561 (2016). doi: 10.1098/rspb.2016.1561; pmid: 27629031
47. M. Burrows, S. R. Shaw, G. P. Sutton, Resilin and chitinous cuticle form a composite structure for energy storage in jumping by froghopper insects. *BMC Biol.* **6**, 41 (2008). doi: 10.1186/1741-7007-6-41; pmid: 18826572
48. M. Burrows, G. P. Sutton, Locusts use a composite of resilin and hard cuticle as an energy store for jumping and kicking. *J. Exp. Biol.* **215**, 3501–3512 (2012). doi: 10.1242/jeb.071993; pmid: 22693029
49. G. P. Sutton, M. Burrows, Biomechanics of jumping in the flea. *J. Exp. Biol.* **214**, 836–847 (2011). doi: 10.1242/jeb.052399; pmid: 21307071
50. S. N. Patek, M. V. Rosario, J. R. A. Taylor, Comparative spring mechanics in mantis shrimp. *J. Exp. Biol.* **216**, 1317–1329 (2013). doi: 10.1242/jeb.078998; pmid: 23239886
51. J. Gosline *et al.*, Elastic proteins: Biological roles and mechanical properties. *Philos. Trans. R. Soc. Lond. B Biol. Sci.* **357**, 121–132 (2002). doi: 10.1098/rstb.2001.1022; pmid: 11911769
52. D. Raabe, C. Sachs, P. Romano, The crustacean exoskeleton as an example of a structurally and mechanically graded biological nanocomposite material. *Acta Mater.* **53**, 4281–4292 (2005). doi: 10.1016/j.actamat.2005.05.027
53. J. F. V. Vincent, Arthropod cuticle: A natural composite shell system. *Compos., Part A Appl. Sci. Manuf.* **33**, 1311–1315 (2002). doi: 10.1016/S1359-835X(02)00167-7
54. D. Klocke, H. Schmitz, Water as a major modulator of the mechanical properties of insect cuticle. *Acta Biomater.* **7**, 2935–2942 (2011). doi: 10.1016/j.actbio.2011.04.004; pmid: 21515418
55. M. V. Rosario, S. N. Patek, Multilevel analysis of elastic morphology: The mantis shrimp's spring. *J. Morphol.* **276**, 1123–1135 (2015). doi: 10.1002/jmor.20398; pmid: 26195244
56. D. W. Haldane, M. M. Plecnik, J. K. Yim, R. S. Fearing, Robotic vertical jumping agility via series-elastic power modulation. *Sci. Robot.* **1**, eaag2048 (2016). doi: 10.1126/scirobotics.aag2048
57. D. Rollinson, S. Ford, B. Brown, H. Choset, in *Proceedings of the ASME 2013 Dynamic Systems and Control Conference.* (ASME, 2013) p. v001T08A002.
58. B. Hopkinson, A method of measuring the pressure produced in the detonation of high explosives or by the impact of bullets. *Phil. Trans. R. Soc. A* **213**, 437–456 (1914). doi: 10.1098/rsta.1914.0010
59. K. W. Hillier, H. Kolsky, An investigation of the dynamic elastic properties of some high polymers. *Proc. Phys. Soc. London. Sect. B* **62**, 111–121 (1949). doi: 10.1088/0370-1301/62/2/304
60. B. Justusson, M. Pankow, C. Heinrich, M. Rudolph, A. M. Waas, Use of a shock tube to determine the bi-axial yield of an aluminum alloy under high rates. *Int. J. Impact Eng.* **58**, 55–65 (2013). doi: 10.1016/j.ijimpeng.2013.01.012
61. J. Yi, M. C. Boyce, G. F. Lee, E. Balizer, Large deformation rate-dependent stress–strain behavior of polyurea and polyurethanes. *Polymer* **47**, 319–329 (2006). doi: 10.1016/j.polymer.2005.10.107
62. G. H. Staab, A. Gilat, A direct-tension split Hopkinson bar for high strain-rate testing. *Exp. Mech.* **31**, 232–235 (1991). doi: 10.1007/BF02326065
63. M. Hudspeth *et al.*, High speed synchrotron x-ray phase contrast imaging of dynamic material response to split Hopkinson bar loading. *Rev. Sci. Instrum.* **84**, 025102 (2013). doi: 10.1063/1.4789780; pmid: 23464246
64. A. D. Mulliken, M. C. Boyce, Mechanics of the rate-dependent elastic–plastic deformation of glassy polymers from low to high strain rates. *Int. J. Solids Struct.* **43**, 1331–1356 (2006). doi: 10.1016/j.ijsolstr.2005.04.016

65. C. C. Chen, J. Y. Chueh, H. Tseng, H. M. Huang, S. Y. Lee, Preparation and characterization of biodegradable PLA polymeric blends. *Biomaterials* **24**, 1167–1173 (2003). doi: 10.1016/S0142-9612(02)00466-0; pmid: 12527257
66. B. Wetzel, P. Rosso, F. Haupert, K. Friedrich, Epoxy nanocomposites: Fracture and toughening mechanisms. *Eng. Fract. Mech.* **73**, 2375–2398 (2006). doi: 10.1016/j.engfracmech.2006.05.018
67. C. R. Siviour, J. L. Jordan, High strain rate mechanics of polymers: A review. *J. Dyn. Behav. Mat.* **2**, 15–32 (2016). doi: 10.1007/s40870-016-0052-8
68. R. B. Bogoslovov, C. M. Roland, Viscoelastic effects on the free retraction of rubber. *J. Appl. Phys.* **102**, 063531 (2007). doi: 10.1063/1.2784018
69. P. H. Mott *et al*., Comparison of the transient stress-strain response of rubber to its linear dynamic behavior. *J. Polym. Sci., B, Polym. Phys.* **49**, 1195–1202 (2011). doi: 10.1002/polb.22292
70. C. C. Lawrence, G. J. Lake, A. G. Thomas, The deformation and fracture of balloons. *Int. J. Non-linear Mech.* **68**, 59–65 (2015). doi: 10.1016/j.ijnonlinmec.2014.08.009
71. J. G. Niemczura, "On the response of rubbers at high strain rates" (Tech. Rep., Sandia National Laboratories, Albuquerque, NM, and Livermore, CA 2010).
72. R. Vermorel, N. Vandenberghe, E. Villermaux, Rubber band recoil. *Proc. R. Soc. A* **463**, 641–658 (2007). doi: 10.1098/rspa.2006.1781
73. L. B. Tunnicliffe, A. G. Thomas, J. J. C. Busfield, The free retraction of natural rubber: A momentum-based model. *Polym. Test.* **47**, 36–41 (2015). doi: 10.1016/j.polymertesting.2015.07.012
74. C. M. Roland, Mechanical behavior of rubber at high strain rates. *Rubber Chem. Technol.* **79**, 429–459 (2006). doi: 10.5254/1.3547945
75. K. Kagaya, S. N. Patek, Feed-forward motor control of ultrafast, ballistic movements. *J. Exp. Biol.* **219**, 319–333 (2016). doi: 10.1242/jeb.130518; pmid: 26643091
76. A. Sakes *et al*., Shooting mechanisms in nature: A systematic review. *PLOS ONE* **11**, e0158277 (2016). doi: 10.1371/journal.pone.0158277; pmid: 27454125
77. M. S. Rodgers, J. J. Allen, K. D. Meeks, B. D. Jensen, S. L. Miller, in *Proceedings of SPIE* (1999), pp. 212–222.
78. R. E. Fischell, L. Wilson, Spacecraft application of subliming materials. *J. Spacecr. Rockets* **2**, 376–379 (1965). doi: 10.2514/3.28187
79. W. Gronenberg, J. Tautz, B. Hölldobler, Fast trap jaws and giant neurons in the ant odontomachus. *Science* **262**, 561–563 (1993). doi: 10.1126/science.262.5133.561; pmid: 17733239
80. Y. Forterre, Slow, fast and furious: Understanding the physics of plant movements. *J. Exp. Bot.* **64**, 4745–4760 (2013). doi: 10.1093/jxb/ert230; pmid: 23913956
81. R. Ritzmann, Snapping behavior of the shrimp *Alpheus californiensis*. *Science* **181**, 459–460 (1973). doi: 10.1126/science.181.4098.459; pmid: 17793337
82. F. Liu *et al*., Asymmetric drop coalescence launches fungal ballistospores with directionality. *J. R. Soc. Interface* **14**, 20170083 (2017). doi: 10.1098/rsif.2017.0083; pmid: 28747394
83. W. J. Heitler, The locust jump. *J. Comp. Physiol.* **89**, 93–104 (1974). doi: 10.1007/BF00696166
84. G. Bonsignori *et al*., The green leafhopper, *Cicadella viridis* (Hemiptera, Auchenorrhyncha, Cicadellidae), jumps with near-constant acceleration. *J. Exp. Biol.* **216**, 1270–1279 (2013). doi: 10.1242/jeb.076083; pmid: 23487271
85. F. C. Moon, *The Machines of Leonardo Da Vinci and Franz Reuleaux: Kinematics of Machines from the Renaissance to the 20th Century* (Springer Science & Business Media, 2007).
86. J. M. Keep, Animal trap, Patent, U.S. Patent Office (1879).
87. M. M. Muñoz, P. S. L. Anderson, S. N. Patek, Mechanical sensitivity and the dynamics of evolutionary rate shifts in biomechanical systems. *Proc. R. Soc. London Ser. B* **284**, 20162325 (2017). doi: 10.1098/rspb.2016.2325; pmid: 28100817
88. T. Claverie, E. Chan, S. N. Patek, Modularity and scaling in fast movements: Power amplification in mantis shrimp. *Evolution* **65**, 443–461 (2011). doi: 10.1111/j.1558-5646.2010.01133.x; pmid: 20840593
89. T. Claverie, S. N. Patek, Modularity and rates of evolutionary change in a power-amplified prey capture system. *Evolution* **67**, 3191–3207 (2013). doi: 10.1111/evo.12185; pmid: 24152002
90. P. S. L. Anderson, D. C. Smith, S. N. Patek, Competing influences on morphological modularity in biomechanical systems: A case study in mantis shrimp. *Evol. Dev.* **18**, 171–181 (2016). doi: 10.1111/ede.12190; pmid: 27161948
91. P. S. L. Anderson, S. N. Patek, Mechanical sensitivity reveals evolutionary dynamics of mechanical systems. *Proc. R. Soc. London Ser. B* **282**, 20143088 (2015). doi: 10.1098/rspb.2014.3088; pmid: 25716791
92. J. Aguilar, A. Lesov, K. Wiesenfeld, D. I. Goldman, Lift-off dynamics in a simple jumping robot. *Phys. Rev. Lett.* **109**, 174301 (2012). doi: 10.1103/PhysRevLett.109.174301; pmid: 23215192
93. N. W. Bartlett *et al*., A 3D-printed, functionally graded soft robot powered by combustion. *Science* **349**, 161–165 (2015). doi: 10.1126/science.aab0129; pmid: 26160940
94. S. Vogel, *Glimpses of Creatures in Their Physical Worlds* (Princeton Univ. Press, Princeton 2009).
95. S. Vogel, Living in a physical world III. Getting up to speed. *J. Biosci.* **30**, 303–312 (2005). doi: 10.1007/BF02703667; pmid: 16052068
96. S. Vogel, Living in a physical world II. The bio-ballistics of small projectiles. *J. Biosci.* **30**, 167–175 (2005). doi: 10.1007/BF02703696; pmid: 15886452
97. H. C. Bennet-Clark, E. C. Lucey, The jump of the flea: A study of the energetics and a model of the mechanism. *J. Exp. Biol.* **47**, 59–67 (1967). pmid: 6058981
98. M. Burrows, M. D. Picker, Jumping mechanisms and performance of pygmy mole crickets (Orthoptera, Tridactylidae). *J. Exp. Biol.* **213**, 2386–2398 (2010). doi: 10.1242/jeb.042192; pmid: 20581268
99. M. Burrows, Jumping performance of froghopper insects. *J. Exp. Biol.* **209**, 4607–4621 (2006). doi: 10.1242/jeb.02539; pmid: 17114396
100. M. Burrows, G. P. Sutton, Pygmy mole crickets jump from water. *Curr. Biol.* **22**, R990–R991 (2012). doi: 10.1016/j.cub.2012.10.045; pmid: 23218011
101. S. E. Bergbreiter, thesis, University of California, Berkeley (2007).
102. L. G. Leal, *Advanced Transport Phenomena: Fluid Mechanics and Convective Transport Processes*, vol. 7 (Cambridge Univ. Press, 2007).
103. T. Nüchter, M. Benoit, U. Engel, S. Ozbek, T. W. Holstein, Nanosecond-scale kinetics of nematocyst discharge. *Curr. Biol.* **16**, R316–R318 (2006). doi: 10.1016/j.cub.2006.03.089; pmid: 16682335
104. E. Purcell, Life at low Reynolds number. *Am. J. Phys.* **45**, 3–11 (1977). doi: 10.1119/1.10903
105. S. Spagnolie, *Complex Fluids in Biological Systems: Experiment, Theory, and Computation* (Springer, New York 2014).
106. A. W. Koch *et al*., Spinalin, a new glycine- and histidine-rich protein in spines of Hydra nematocysts. *J. Cell Sci.* **111**, 1545–1554 (1998). pmid: 9580562
107. A. Pringle, S. N. Patek, M. Fischer, J. Stolze, N. P. Money, The captured launch of a ballistospore. *Mycologia* **97**, 866–871 (2005). doi: 10.1080/15572536.2006.11832777; pmid: 16457355
108. J. Edwards, D. Whitaker, S. Klionsky, M. J. Laskowski, Botany: A record-breaking pollen catapult. *Nature* **435**, 164 (2005). doi: 10.1038/4351164a; pmid: 15889081
109. D. L. Whitaker, L. A. Webster, J. Edwards, The biomechanics of *Cornus canadensis* stamens are ideal for catapulting pollen vertically. *Funct. Ecol.* **21**, 219–225 (2007). doi: 10.1111/j.1365-2435.2007.01249.x
110. S. N. Patek, J. E. Baio, B. L. Fisher, A. V. Suarez, Multifunctionality and mechanical origins: Ballistic jaw propulsion in trap-jaw ants. *Proc. Natl. Acad. Sci. U.S.A.* **103**, 12787–12792 (2006). doi: 10.1073/pnas.0604290103; pmid: 16924120
111. M. Burrows, Jumping mechanisms in jumping plant lice (Hemiptera, Sternorrhyncha, Psyllidae). *J. Exp. Biol.* **215**, 3612–3621 (2012). doi: 10.1242/jeb.074682; pmid: 22771753
112. M. J. McHenry *et al*., The comparative hydrodynamics of rapid rotation by predatory appendages. *J. Exp. Biol.* **219**, 3399–3411 (2016). doi: 10.1242/jeb.140590; pmid: 27807217
113. R. S. James, R. S. Wilson, Explosive jumping: Extreme morphological and physiological specializations of Australian rocket frogs (*Litoria nasuta*). *Physiol. Biochem. Zool.* **81**, 176–185 (2008). doi: 10.1086/525290; pmid: 18190283
114. C. V. Anderson, T. Sheridan, S. M. Deban, Scaling of the ballistic tongue apparatus in chameleons. *J. Morphol.* **273**, 1214–1226 (2012). doi: 10.1002/jmor.20053; pmid: 22730103
115. C. V. Anderson, Off like a shot: Scaling of ballistic tongue projection reveals extremely high performance in small chameleons. *Sci. Rep.* **6**, 18625 (2016). doi: 10.1038/srep18625; pmid: 26725508
116. H. C. Bennet-Clark, The energetics of the jump of the locust *Schistocerca gregaria*. *J. Exp. Biol.* **63**, 53–83 (1975). pmid: 1159370
117. A. P. Gerratt, S. Bergbreiter, Incorporating compliant elastomers for jumping locomotion in microrobots. *Smart Mater. Struct.* **22**, 014010 (2013). doi: 10.1088/0964-1726/22/1/014010
118. A. Debray, Manipulators inspired by the tongue of the chameleon. *Bioinspir. Biomim.* **6**, 026002 (2011). doi: 10.1088/1748-3182/6/2/026002; pmid: 21422504
119. J. S. Koh, S. P. Jung, M. Noh, S. W. Kim, K. J. Cho, in *IEEE International Conference on Robotics and Automation* (IEEE, 2013), pp. 26–31.
120. J. Zhao *et al*., MSU Jumper: A single-motor-actuated miniature steerable jumping robot. *IEEE Trans. Robot.* **29**, 602–614 (2013). doi: 10.1109/TRO.2013.2249371
121. P. Weiss, Hop... Hop... Hopbots! *Sci. News* **159**, 88–91 (2001). doi: 10.2307/3981566
122. J. German, Sandia-developed intelligent software agents challenge electronic intruders. *Sandia Lab News* **52**(10), LN05-19-00 (19 May 2000); http://www.sandia.gov/LabNews/LN05-19-00/software_story.html.
123. S. N. Patek, B. N. Nowroozi, J. E. Baio, R. L. Caldwell, A. P. Summers, Linkage mechanics and power amplification of the mantis shrimp's strike. *J. Exp. Biol.* **210**, 3677–3688 (2007). doi: 10.1242/jeb.006486; pmid: 17921168
124. M. Versluis, B. Schmitz, A. von der Heydt, D. Lohse, How snapping shrimp snap: Through cavitating bubbles. *Science* **289**, 2114–2117 (2000). doi: 10.1126/science.289.5487.2114; pmid: 11000111
125. H. C. Astley, T. J. Roberts, Evidence for a vertebrate catapult: Elastic energy storage in the plantaris tendon during frog jumping. *Biol. Lett.* **8**, 386–389 (2012). doi: 10.1098/rsbl.2011.0982; pmid: 22090204
126. H. C. Astley, T. J. Roberts, The mechanics of elastic loading and recoil in anuran jumping. *J. Exp. Biol.* **217**, 4372–4378 (2014). doi: 10.1242/jeb.110296; pmid: 25520385
127. X. Noblin, S. Yang, J. Dumais, Surface tension propulsion of fungal spores. *J. Exp. Biol.* **212**, 2835–2843 (2009). doi: 10.1242/jeb.029975; pmid: 19684219
128. L. Mahadevan, P. Matsudaira, Motility powered by supramolecular springs and ratchets. *Science* **288**, 95–99 (2000). doi: 10.1126/science.288.5463.95; pmid: 10753126
129. J. H. de Groot, J. L. van Leeuwen, Evidence for an elastic projection mechanism in the chameleon tongue. *Proc. R. Soc. London Ser. B* **271**, 761–770 (2004). doi: 10.1098/rspb.2003.2637; pmid: 15209111
130. U. K. Müller, S. Kranenbarg, Power at the tip of the tongue. *Science* **304**, 217–219 (2004). doi: 10.1126/science.1097894; pmid: 15073361

ACKNOWLEDGMENTS

We thank A. Guo, M. Muñoz, R. Orszulik, and B. Perlman for comments and assistance. **Funding:** This material is based on work supported by the U.S. Army Research Laboratory and the U.S. Army Research Office under contract/grant number W911NF-15-1-0358. Additional support was provided by the Royal Society (UF130507 to G.P.S.), NSF (IOS-1439850 to S.N.P.), and the John Simon Guggenheim Foundation (to S.N.P.). **Author contributions:** All authors conceived the project and were involved with revising and editing the manuscript. M.I., S.M.C., A.J.C., X.M., S.B., and S.N.P. contributed to the methodology. M.S.B., L.L.F., X.M., S.M.C., Y.K., J.-s.K., S.N.P., S.B., M.I., C.-Y.K., and F.Z.T. collected and compiled the data. M.I., S.M.C., E.A., S.B., and S.N.P. wrote the manuscript. **Competing interests:** All authors declare no competing interest. **Data availability:** The data and analyses reported in this paper are presented in the manuscript and supplementary materials.

SUPPLEMENTARY MATERIALS

www.sciencemag.org/content/360/6387/eaao1082/suppl/DC1
Supplementary Text
Figs. S1 to S12
Tables S1 to S3
References (*131*–*165*)

14 June 2017; accepted 7 March 2018
10.1126/science.aao1082

The principles of cascading power limits in small, fast biological and engineered systems

Mark Ilton, M. Saad Bhamla, Xiaotian Ma, Suzanne M. Cox, Leah L. Fitchett, Yongjin Kim, Je-sung Koh, Deepak Krishnamurthy, Chi-Yun Kuo, Fatma Zeynep Temel, Alfred J. Crosby, Manu Prakash, Gregory P. Sutton, Robert J. Wood, Emanuel Azizi, Sarah Bergbreiter and S. N. Patek

Science **360** (6387), eaao1082.
DOI: 10.1126/science.aao1082

Hop, skip, jump, or massive leap

In biological and engineered systems, an inherent trade-off exists between the force and velocity that can be delivered by a muscle, spring, or combination of the two. However, one can amplify the maximum throwing power of an arm by storing the energy in a bow or sling shot with a latch mechanism for sudden release. Ilton *et al.* used modeling to explore the performance of motor-driven versus spring-latch systems in engineering and biology across size scales. They found a range of general principles that are common to animals, plants, fungi, and machines that use elastic structures to maximize kinetic energy.

Science, this issue p. eaao1082